[3]See, for instance, the review article by H. L. Frisch, Advan. Chem. Phys. 5, 229 (1964).
[4]W. G. Hoover and A. G. DeRocco, J. Chem. Phys. 36, 3149 (1961).
[5]W. G. Hoover, J. Chem. Phys. 40, 937 (1964).
[6]H. Reiss, H. L. Frisch, and J. L. Lebowitz, J. Chem. Phys. 31, 369 (1959).
[7]M. Cotter and H. L. Frisch, J. Chem. Phys. 57, 1011 (1972).
[8]R. Becker and W. Döring, Ann. Physik 24, 719 (1935).
[9]J. E. Mayer and Wm. W. Wood, J. Chem. Phys. 42, 12 (1965).
[10]W. G. Hoover and B. J. Alder, J. Chem. Phys. 46, 686 (1967).

PHYSICAL REVIEW A VOLUME 7, NUMBER 1 JANUARY 1973

Comparison of Experiments with the Modified Mode-Mode Coupling Theory of Kawasaki in Binary Fluids*

B. Chu,† S. P. Lee, and W. Tscharnuter
Chemistry Department, State University of New York at Stony Brook, Stony Brook, New York 11790
(Received 7 June 1972; revised manuscript received 27 July 1972)

Linewidth, angular dissymmetry, and hydrodynamic-shear-viscosity data of a critical binary-liquid mixture of isobutyric acid in water compares well with the modified mode-mode coupling theory of Kawasaki in the range $11 \geq K\xi \geq 0.0067$ after corrections for vertex, nonlocal shear viscosity and deviation of the Ornstein–Zernike correlation function. Deviations between experiments and theory in the critical region ($K\xi > 4$) suggest needs for further improvements in theory at large values of $K\xi$ as well as measurements of the hydrodynamic shear viscosity at small temperature distances from the critical mixing point.

I. INTRODUCTION AND THEORETICAL BACKGROUND

The first measurements of Rayleigh linewidths for binary fluids were reported by Alpert and coworkers.[1] Their data were explained by Debye[2] who extended the Landau–Placzek theory[3] to concentration fluctuations in a binary-liquid mixture by considering the diffusion broadening as a reflection from standing concentration waves which obey the Bragg relation $K = ks$ with $k = 2\pi/\lambda$ and $s = 2\sin\frac{1}{2}\theta$; λ and θ being the wavelength of light in the medium and the scattering angle, respectively.

In the hydrodynamic region ($K\xi \ll 1$ with ξ being the long-range correlation length), the Landau–Placzek and Debye equation predicts that the power spectrum of the central component due to concentration fluctuations is a Lorentzian-shaped line of half-width Γ:

$$\Gamma = \chi K^2 \quad \text{(simple fluid)}, \tag{1a}$$

$$\Gamma = DK^2 \quad \text{(binary fluid)}, \tag{1b}$$

where χ and D are the thermal-diffusivity and the mutual-diffusion coefficients, respectively. The mutual-diffusion coefficient D is given by $D \equiv \alpha^* \times (\partial\mu/\partial c)_{P,T}$, where α^* is the transport (or Onsager kinetic) coefficient, which is sometimes referred to as the concentration conductivity, relating the diffusion coefficient to $(\partial\mu/\partial c)_{P,T}$ with μ as the chemical potential and c the concentration.

In the nonlocal hydrodynamic region ($\xi K \leq 1$), Fixman[4] and Felderhof[5] first extended the Landau–Placzek–Debye theory to include the effect of long-range correlation. According to the mode-mode coupling theory developed by Kadanoff and Swift[6] and then further extended by Kawasaki,[7] the Rayleigh linewidth in the nonlocal hydrodynamic region ($K\xi \leq 1$) has the form

$$\Gamma = DK^2(1 + \tfrac{3}{5}K^2\xi^2) \ , \tag{2}$$

where $D = k_B T/6\pi\eta^*_{hf}\xi$, with η^*_{hf} and k_B being the high-frequency shear viscosity and the Boltzmann constant, respectively. The Kawasaki equation for the decay rate Γ with the wave vector $\vec{K}$ is applicable to all values of $K\xi (\equiv X)$:

$$\Gamma_K = (8A/3\pi)\xi^{-3}H_0(X) \ , \tag{3}$$

where $A \equiv k_B T/16\eta^*_{hf}$ and the function $H_0(X)$ is given by

$$H_0(X) = \tfrac{3}{4}\left[1 + X^2 + (X^3 - X^{-1})\arctan X\right] \ . \tag{4}$$

In the critical region ($\xi K > 1$) $\Gamma_K = AK^3$, while Eq. (3) reduces to Eq. (1) for $\xi K \ll 1$.

Decay rates of order-parameter fluctuations near the critical point of fluids have been extensively investigated by means of optical self-beating spectroscopy.[8] It has been shown that Eq. (3) is applicable to only the singular part of thermodynamic properties,[9,10] and that nondivergent background contributions must be taken into account in comparing theory with experiments. For a binary-fluid mixture, the nondivergent background contribution is crucial when the system is far from the critical point even though the contribution becomes negligibly small in the critical region. We shall

include the nondivergent background contributions, especially those related to the high-frequency shear viscosity η^*_{hf} in comparison of our experiments with theory. Furthermore, Eq. (3) can be modified to take into account (a) deviations from the Ornstein–Zernike form of the correlation function, [11] (b) vertex corrections, [12] and (c) the nonlocality of the high-frequency shear viscosity $\eta^*_{hf}(K\xi)$. [13]

We have reinvestigated the spectral width of light scattered by concentration fluctuations near the critical mixing point of isobutyric acid in water using the technique of time-dependent photocurrent signal correlation. [14] These data together with intensity[15] and viscosity[16,17] results of the same system are compared with Eq. (3) and its modifications. A preliminary analysis has been published elsewhere. [18] In this article we wish to report a more detailed comparison of theory with all of our linewidth results on the isobutyric-acid–water system which we have measured thus far by means of signal correlation.

II. EXPERIMENTAL METHODS

A. Sample Preparation

Isobutyric acid (Fisher certified reagent grade) was purified by preparative gas chromatography using a 20-ft. -long$\times\frac{3}{8}$-in. o.d. column packed with 30% FFAP on 60-80 chromosorb *P*. A 38.6-wt% isobutyric acid in deionized doubly distilled water was sealed in an 8-mm i.d. cylindrical glass light-scattering cell. The phase-separation temperature (T_c) was determined to be 26.08 °C by visual observation. This value of the critical temperature is in reasonable agreement with the best in the literature. [15–17] On a relative scale, we have determined our critical temperature to within 0.001 °C.

B. Laser Self-Beating Spectrometer

Our laser spectrometer is a modified version of the one described elsewhere. [15,19] We have in essence used three different spectrometers of slightly different optical geometry consisting of varying sizes of angular and field stops as well as lasers of different output powers. For measurements in the very immediate neighborhood of the critical mixing point, a dc-excited He-Ne cw gas laser with an output power of about 2 mW at 632.8 nm was used. As we moved away from the critical mixing point, higher-power lasers were used to ensure a good signal-to-noise ratio of our measurements. We used two dc-excited He-Ne cw gas lasers at 632.8 nm with output powers of 15 and 60 mW as well as an argon-ion laser of 200-mW output power at 488 nm. The light beams were focused to about a 0.2-mm diam. Time-dependent photocurrents from S-20 photomultipliers, such as EMI 9558B and ITT FW130, were amplified and analyzed with a SAICOR signal correlator which was interfaced with an IBM 1800 digital computer for direct data acquisition. [20] The SAICOR correlator accepted an analog photocurrent signal and then converted its amplitude into digital information. All subsequent processes were performed digitally. Alignments of the spectrometers were checked first with a centrifuged aqueous solution of colloidal silica (LUDOX) which showed a constant scattered intensity for vertically polarized incident light to within 1–2% over an angular range of 20°–140° depending on the spectrometers. Linewidth measurements from dilute solutions of polystyrene latex spheres with sizes 0.0907 ± 0.0056 (run No. LS-1132-B) and 0.357 ± 0.0056 μ (run No. LS-1010-E) obeyed the Stokes–Einstein relation $\Gamma = (k_B T/6\pi\eta^* r) \times K^2$ with r and η^* being the radius of the latex spheres and the hydrodynamic shear viscosity, respectively. We also found that calibrations furnished by the Dow Chemical Co. for the above two latex samples were different from both our linewidth measurements and our own electron microscopic studies using two different electron microscopes and each with two different magnifications. The details of our calibration will be published elsewhere. In summary, we are able to measure the mutual-diffusion coefficients to an accuracy of ± 1% or better.

The signal correlator measured the time-dependent photocurrent autocorrelation function. A total of 505 linewidths were measured at the critical solution concentration in the temperature interval $(0.003 \leq T - T_c \leq 30)$ °C for scattering angles varying from 20° to 140°. Temperature of the sample was controlled to better than 0.001 °C for measurements very near the critical mixing point ($T - T_c < 0.02$ °C) and to ± 0.03 °C for those at large temperature distances ($T - T_c > 3$ °C). Each linewidth was obtained from a 95–100 point three-parameter least-squares fit of the exponential photocurrent autocorrelation function $C_s(t)$ to a rms fitting error of ± (0.5–1)% according to the equation $C_s(t) = Ae^{-2\Gamma|t|} + B$, where the three parameters are A, B, and Γ. When there was no baseline drift, the correlator output was least-squares fitted to $Ae^{-2\Gamma|t|}$ with a known B. The two approaches invariably gave us the same result. In fitting the photocurrent autocorrelation function with a single exponential, we have not implicitly assumed that critical concentration fluctuations can be represented by a single decay rate Γ. Rather, we have made several very careful linewidth measurements and found that the least-squares fitting of one single exponential function already leads to an agreement between data experiment and theory to better than 0.5% over many linewidths. It should also be noted that our 505 linewidths correspond to over 50 000 delay point

measurements. Thus the data would probably represent more than an entire year of measurement time if older methods[21] were used.

III. RESULTS AND DISCUSSION

A. Critical Region ($\xi K > 1$)

Halperin and Hohenberg[22] proposed that $\Gamma = K^z F(K\xi)$, where Z is the degree of homogeneity, and a specific form of $F(K\xi)$ was derived first by Kawasaki[7] and subsequently by Ferrell.[23] According to Kawasaki,[7] $\Gamma = AK^3$ in the critical region. Figure 1 shows a typical plot of $\ln\Gamma$ vs $\ln K$ at $T - T_c = 0.006$ °C. Least-squares fits of 37 linewidths at $T - T_c = 0.003$ °C and of 30 linewidths at $T - T_c = 0.006$ °C give $\Gamma = (1.075 \pm 3.4\%) \times 10^{-13} K^{[2.976 \pm 1.5\%]}$ rad/sec and $(1.028 \pm 2.3\%) \times 10^{-13} K^{[3.046 \pm 1.0\%]}$ rad/sec, respectively. Thus, we find that Z is indeed equal to 3 and that background contributions must be negligibly small in the critical region since the Kawasaki equation represents only the singular part of the linewidth exhibiting the asymptotic critical behavior. We have intentionally made linewidth measurements at various scattering angles, but at *fixed* temperatures above the critical temperature satisfying the condition $\xi K > 2$. With $A = k_B T/16\eta^*_{hf}$ and $Z = 3$, we have computed the so-called high-frequency shear viscosity which is assumed to be independent of $K\xi$. It should be noted that if η^*_{hf} depends upon $K\xi$, then $\Gamma = AK^3$ cannot be strictly correct over large ranges of $K\xi$. Table I shows a comparison of $\bar{\eta}^*_{hf}$ $(= k_B T/16A)$ and the measured hydrodynamic shear viscosity by means of the classical capillary method.[17] We find $\bar{\eta}^*_{hf} < \eta^*$ and $\bar{\eta}^*_{hf}$ depends upon temperature. The superscript bar is used to emphasize the fact that our $\bar{\eta}^*_{hf}$ is averaged over ranges of $K\xi$ if η^*_{hf} depends upon $K\xi$. In Table I, if we take the actual measured hydrodynamic shear viscosity, we find that $\eta^*/\bar{\eta}^*_{hf}$ decreases as the critical mixing point is approached. The decrease suggests a very weak maximum in $\eta^*/\bar{\eta}^*_{hf}$ since $\eta^* \simeq 1.07\eta^*_{hf}$ in the hydrodynamic limit. Such a maximum is contrary to the usual expectation. Furthermore, $\eta^*_c/\bar{\eta}^*_{hf}$ is relatively constant, if not with a slightly increasing trend as the critical mixing point is approached. η^*_c represents the computed hydrodynamic shear viscosity using the formula[24]

$$\eta^*_c = (E/\alpha)(\epsilon^{-\alpha} - 1) + F\epsilon + G \ , \qquad (5)$$

with $\epsilon = (T - T_c)/T_c$. Values of parameters E, F, G, and α are listed in Table II. For η^*_c in Table I, $E = 0.27 \pm 0.04$, $F = -10.0 \pm 0.8$, $G = 1.35 \pm 0.10$, and $\alpha = -0.117 \pm 0.019$, as reported by Allegra, Stein, and Allen,[17] were used. In our analysis of their data, we believe that Allegra, Stein, and Allen[17] have essentially excluded their viscosity measurements in the critical region in order to obtain the reported values of those parameters. Since the capillary method is susceptible to error for measurements in the very immediate neighborhood of the critical mixing point because of gravitational effects, it is quite conceivable that the maximum in $\eta^*/\bar{\eta}^*_{hf}$ is an experimental artifact of the capillary method. We shall accept the finding that the ratio of the hydrodynamic shear viscosity to the ($K\xi$-averaged) Kawasaki high-frequency viscosity is about 1.23 in the critical region, and perhaps the deviation increases as the critical mixing point is approached since $\eta^*/\bar{\eta}^*_{hf}$ at $T - T_c = 0.025$ °C is least reliable because of limited angular range available for $\xi K > 1$ at that temperature distance from the critical mixing point.

TABLE I. Comparison of the Kawasaki high-frequency viscosity and the hydrodynamic shear viscosity in the critical region for the critical binary mixture of isobutyric acid in water.

$T - T_c$ (°C)	No. Γ measured	A (10^{-13} cm^3/sec)	$\bar{\eta}^*_{hf}$ (cP)	$\eta^*/\bar{\eta}^*_{hf}$ [a]	$\eta^*_c/\bar{\eta}^*_{hf}$ [b]
0.003	37	$1.054 \pm 0.3\%$[c]	2.45	1.19	1.25
0.006	30	$1.065 \pm 0.3\%$[c]	2.42	1.20	1.24
0.009	22	1.07	2.41	1.20	1.23
0.025	15	1.12	2.32	1.24	1.25

[a] η^* interpolated from measured values of η^* by Allegra, Stein, and Allen (Ref. 17).

[b] η^*_c computed using the formula $\eta^*_c = (E/\alpha)(\epsilon^{-\alpha} - 1) + F\epsilon + G$; 10^{-2} g/cm sec with $E = 0.27 \pm 0.04$, $F = -10.0 \pm 0.8$, $G = 1.35 \pm 0.10$, and $\alpha = -0.117 \pm 0.019$ as reported by Allegra, Stein, and Allen (Ref. 17). $\epsilon = (T - T_c)/T_c$.

[c] $\pm 0.3\%$ represents the standard deviation of our measurements when we take $Z = 3$.

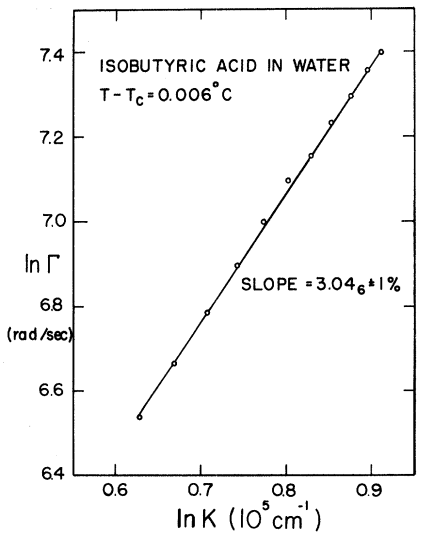

FIG. 1. Log-log plot of the decay rate Γ as a function of K at $T - T_c = 0.006$ °C. Γ (rad/sec) $= (1.028 \pm 2.3\%) \times 10^{-13} K^{[3.046 \pm 1.0\%]}$ with K expressed in cm^{-1}.

TABLE II. Least-squares fits of viscosity data according to Eq. (5) for the isobutyric-acid–water system.

Method	No. data points	Temperature range (°C)	E	F	G	α
Γ	17[a]	$0.100 \leq T - T_c \leq 30.0$	3.42 ± 2.93	1.37 ± 6.31	-3.74 ± 3.92	-0.541 ± 0.134
Γ	18[a]	$0.075 \leq T - T_c \leq 30.0$	1.40 ± 1.31	-3.33 ± 4.53	-0.894 ± 2.11	-0.388 ± 0.152
Capillary	Ref. b		1.33 ± 0.4	-3.3 ± 1.4	-0.68 ± 0.04	-0.37 ± 0.04
Capillary	Ref. c		0.27 ± 0.04	-10.0 ± 0.8	1.35 ± 0.10	-0.117 ± 0.019
Capillary	25[d]	$0.002 \leq T - T_c \leq 8.32$	1.03 ± 0.258	-0.928 ± 2.82	-0.357 ± 0.529	-0.304 ± 0.030
Capillary	18[e]	$0.076 \leq T - T_c \leq 8.32$	0.19 ± 0.028	-11.4 ± 0.67	1.57 ± 0.08	-0.067 ± 0.021

[a] $\eta_{hf}^* = k_B T / 6\pi D\xi$. Actual data listed in Table III. Only the η_{hf}^* value at $T - T_c = 0.075$ °C is omitted for the fitting with 17 data points.

[b] Data of Woermann and Sarholz (Ref. 16) as fitted by Allegra, Stein, and Allen (Ref. 17).

[c] Data of Allegra, Stein, and Allen (Ref. 17) as fitted by Allegra, Stein, and Allen (Ref. 17).

[d] Data of Allegra, Stein, and Allen, their Table II, as fitted by us.

[e] Data of Allegra, Stein, and Allen, their Table II, but excluding point Nos. 1–7, as fitted by us.

The parameters in Eq. (5) are very sensitive to minor variations in experimental data. In Table II, we note that η_{hf}^* ($= k_B T / 6\pi D\xi$ in the hydrodynamic limit) can be represented by quite different parameters whether we use 17 or 18 data points for the least-squares fit of Eq. (5). Similarly, if we use all the 25 data points of the viscosity data of Allegra, Stein, and Allen,[17] we obtain parameter values different from those reported by Allegra, Stein, and Allen. Figure 2 represents a deviation plot for viscosities calculated from Eq. (5) using the 25 data points. It is interesting to note that reasonably good agreement can be obtained from seemingly different parameters. The four-parameter equation requires data of ultra-high precision. It is likely that our measurements and even those of hydrodynamic shear viscosity are not sufficiently precise for an unambiguous fit by means of Eq. (5). On the other hand, all the experimental data point toward a range of α between -1 and 0. Thus, the presence of a cusp in the critical viscosity anomaly is indicated.

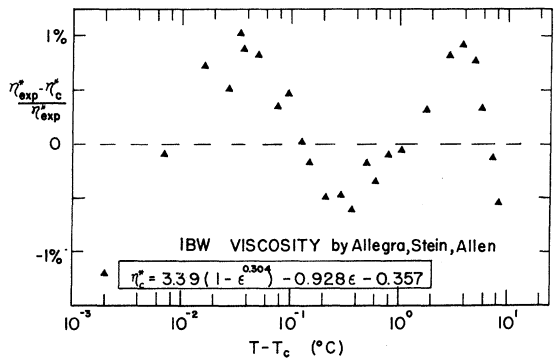

FIG. 2. Deviation plot for high-frequency viscosities calculated from Eq. (5) using $E = 1.03 \pm 0.258$, $F = -0.928 \pm 2.82$, $G = -0.357 \pm 0.529$, and $\alpha = -0.304 \pm 0.031$.

B. Nonlocal Hydrodynamic Region ($\xi K \geq 1$)

In the nonlocal hydrodynamic region the Rayleigh linewidth obeys Eq. (2) as shown in Fig. 3. From a plot of Γ/K^2 vs K^2, we obtain the mutual-diffusion coefficient D from the intercept. The results are tabulated in Table III. We have also computed the diffusion coefficient at temperature distances very near the critical mixing temperature by means of the Kawasaki–Stokes–Einstein relation

$$D = k_B T / 6\pi \eta_{hf}^* \xi \ , \tag{6}$$

where the long-range correlation length ξ is obtained from a least-squares fit of the intensity data,[15] with

$$\xi = (0.357 \pm 0.007) \times 10^{-7} \epsilon^{-0.613 \pm 0.001} \text{ cm} \tag{7}$$

and

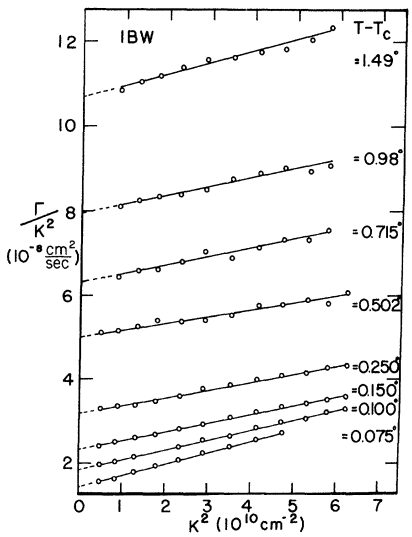

FIG. 3. Plot of Γ/K^2 vs K^2 in the nonlocal hydrodynamic region.

TABLE III. Mutual-diffusion coefficient of 38.6-wt. % isobutyric acid in water from Rayleigh linewidth measurements.[a]

$T-T_c$ (°C)	$D(=\lim_{K\to u}\Gamma/K^2)$ (10^{-8} cm^2/sec)	D ($\equiv k_BT/6\pi\eta^*_{ht}\xi$)[b] ($10^{-8}$ cm^2/sec)
0.003		0.217
0.006		0.335
0.009		0.431
0.025		0.841
0.075	1.44(4)	
0.100	1.86(9)	
0.150	2.36(1)	
0.250	3.21(2)	
0.348	3.94(6)	
0.502	5.06(4)	
0.715	6.35(5)	
0.98	7.95(4)	
1.39	10.7(2)	
2.47	15.3(6)	
3.45	20.0(0)	
5.01	26.3(4)	
7.15	36.7(0)	
9.00	44.2(5)	
10.95	52.6(8)	
15.00	73.1(4)	
20.00	101.(3)	
30.00	186.(4)	

[a]The values for $k_BT/6\pi\eta^*\xi$ have been reported (Ref. 18). In general, we find $6\pi\eta^*\xi D/k_BT$ varies from 1.05 to 1.08.

[b]ξ obtained from a least-squares fit of the intensity data (Ref. 15) with $\xi = (0.35(7) \pm 0.007) \times 10^{-7}\epsilon^{-0.613\pm0.001}$ cm.

$\eta^*_{ht} = k_BT/16A$ from a least-squares fit of $\Gamma = AK^3$. Figure 4 shows a plot of $\ln D$ vs $\ln(T-T_c)$. The plot clearly indicates that the temperature dependence of the diffusion coefficient *cannot* be represented by a simple exponent, such as $D \propto \epsilon^{\gamma^*}$. Furthermore, a discrepancy is observed for D ($= k_BT/6\pi\overline{\eta}^*_{ht}\xi$) and the values extrapolated from $D = \lim_{k\to 0}\Gamma/K^2$ very near the critical mixing point. The same manifestation is shown in Table I where $\eta^*/\overline{\eta}^*_{ht} \simeq 1.23$ for small temperature distances from the critical point, while $\eta^*/\overline{\eta}^*_{ht} \simeq 1.07$ at large temperature distances.[18] Independently, Kawasaki and Lo[13] have computed an explicit correction factor to account for the $K\xi$ dependence of the high-frequency shear viscosity. We shall discuss the nonlocal shear viscosity together with all the other corrections.

The long-range correlation length ξ_Γ can be computed from the ratio of slope/intercept of the isotherms in Fig. 3. The subscript Γ denotes the value of ξ obtained by means of Eq. (2). Table IV shows a comparison of ξ_Γ with those from the angular distribution of scattered intensity [Eq. (7)]. Over a limited temperature range ($0.075 \leq T - T_c \leq 0.150$) °C we can identify the same correlation length ξ which governs the critical behaviors of both static and dynamic properties of the critical binary fluid. Even the factor $\frac{3}{5}$ in Eq. (2) is properly obeyed. However, ξ_Γ appears to have a somewhat different temperature dependence with $\nu_\Gamma < 0.6$. The discrepancy between ν_Γ and ν could probably be attributed to the nonlocality in η^*_{ht}. Then, Eq. (2) cannot be used for determining ξ_Γ over large ranges of $K\xi$ at many different temperature distances from the critical mixing point. Thus, the ξ values represented by Eq. (7) are more reliable than those from the linewidth measurement. If we combine the intensity data measured at $\lambda_0 = 435.8$ nm with those measured at $\lambda_0 = 632.8$ nm, we

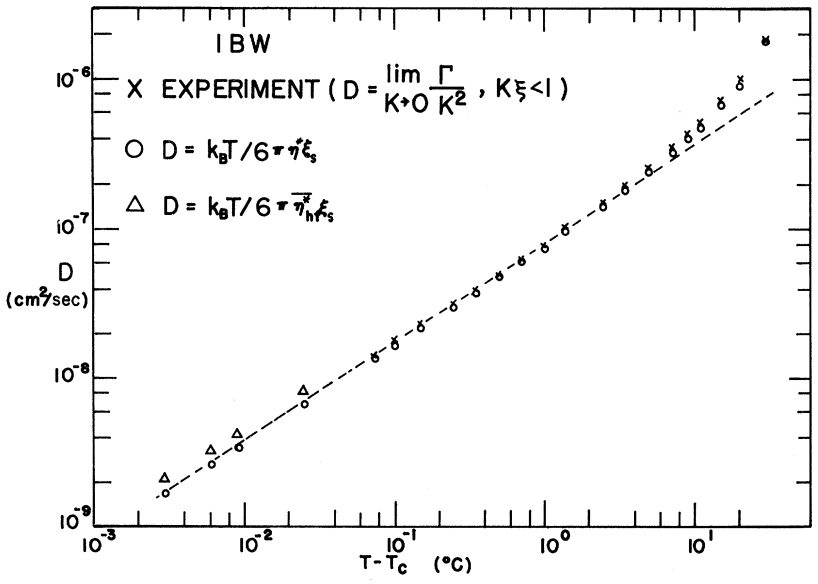

FIG. 4. Temperature dependence of the diffusion coefficient in a critical binary-liquid mixture. Note: The dotted straight line is obtained by joining data points in the temperature range ($0.075 < T - T_c < 1.0$) °C in order to show deviations from the simple exponent behavior [$D \propto \epsilon^{\gamma^*}$, where $\epsilon = (T-T_c)/T_c$ and γ^* is an *apparent* exponent] at both large and small temperature distances, but for different reasons. Note: The difference between 0 and X is real. The (Δ) values from $D = k_BT/6\pi\overline{\eta}^*_{ht}\xi$ are distinctly higher than the extrapolated dotted line indicating a discrepancy between experiment and theory.

TABLE IV. Long-range correlation length ξ from measurements of angular distribution of spectral width and that of scattered intensity for the isobutyric-acid–water system.

$T-T_c$ (°C)	ξ_Γ (Å)	ξ [a] (Å)	ξ_Γ/ξ (=1)
0.075	562	574	0.98
0.100	460	482	0.96
0.150	381	376	1.01
0.250	311	275	1.13
0.348	260	224	1.16

[a] $\xi = \xi_0 \epsilon^{-\nu}$ with $\xi_0 = (0.357 \pm 0.007) \times 10^{-7}$ cm and $\nu = 0.613 \pm 0.001$. The data were those from Ref. 15 using a wavelength of 435.8 nm with a medium pressure mercury-arc lamp.

get

$$\xi = (0.362 \pm 0.010) \times 10^{-7} \epsilon^{-0.618 \pm 0.015} \text{ cm} .$$

It should be noted that the uncertainties are rms fitting errors, not estimates of accuracy. Thus we find $\nu = 0.613 \pm 0.001$ using one set of measurements and $\nu = 0.618 \pm 0.015$ when we include additional intensity data which are slightly poorer in quality. We have decided not to make accuracy estimates on the critical exponents as too many unknown factors could be involved. Rather, we have tried to report two values using independent data measured at different times. If pressed, we believe that the most probable value for ν from our intensity studies is 0.615 ± 0.015. The literature is filled with critical exponent determinations, quoting far better accuracy estimates which we do not take very seriously. On the other hand, the uncertainties on Γ should be considered from a slightly different viewpoint since we have calibrated our instruments using latex spheres of known diameters. Our calibrations have shown that we can measure Γ to an accuracy of $\pm 1\%$ or better.

C. Kawasaki Theory and Modifications

The Kawasaki theory [Eqs. (3) and (4)] disagrees with experimental data as shown in Fig. 5 because η^*_{hf} is assumed to be independent of temperature. Equation (5) further shows that a simple separation of the form

$$D = D_0 + k_B T / 6\pi\eta^*_{hf}\xi \qquad (8)$$

(with η^*_{hf} as a constant) is inappropriate. Yet, we see that $\Gamma = AK^3$ holds very well at constant temperatures suggesting a negligible background in the critical region. Thus, our approach is to try to compare the Kawasaki theory by taking into account (a) the vertex correction, (b) the approximate Ornstein–Zernike form of the correlation function in the Kawasaki equation, and (c) the nonlocal shear viscosity. Before we consider the modifications, it is interesting to note that we can obtain a three-parameter fit of the Kawasaki equation as shown in Fig. 6. The agreement between the computed curve and experimental data is very good.

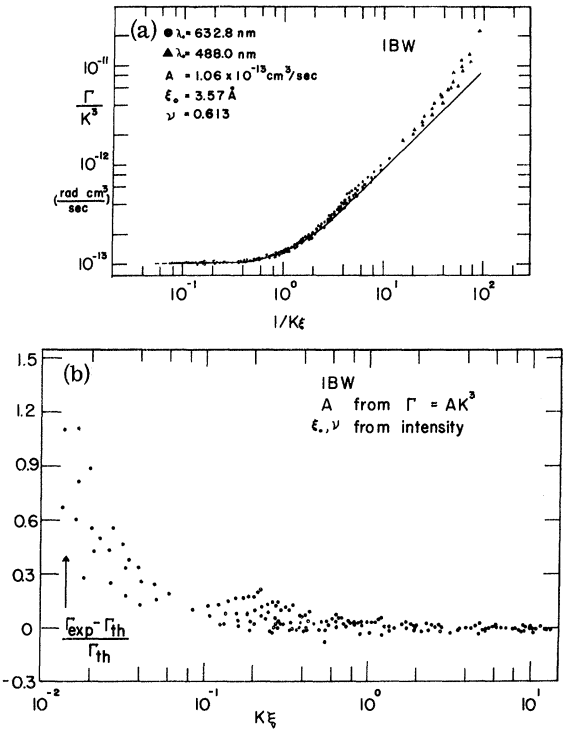

FIG. 5. Comparison of the Kawasaki theory with the linewidth data for the isobutyric-acid–water system at the critical solution concentration. (a) A plot of the Kawasaki linewidth with $A = 1.06 \times 10^{-13}$ cm^3/sec, $\nu = 0.613$, and $\xi_0 = (0.357 \pm 0.007) \times 10^{-7}$ cm. (b) A plot of the deviation of the isobutyric-acid–water linewidth data from the theoretical curve [Eq. (3)] with parameters shown in (a).

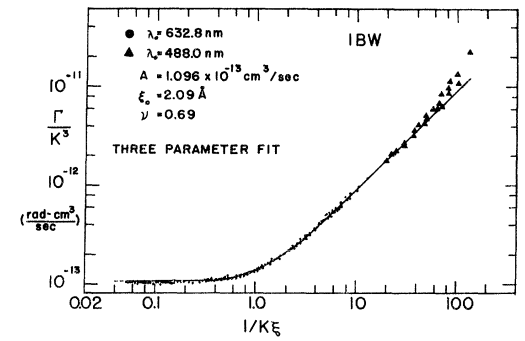

FIG. 6. Least-squares fit of the Kawasaki equation [Eqs. (3) and (4)] with experimental data. The average parameters $A = 1.096 \times 10^{-13}$ cm^3/sec, $\nu = 0.69$, and $\xi_0 = 0.209 \times 10^{-7}$ cm represent distorted values because of the forced fit.

The difficulty lies with disagreements of the values of parameters obtained this way and by other methods.

1. Vertex Correction

The contributions of the simplest vertex corrections[12] on the decay rate Γ are -2.44% for $\xi K \ll 1$ and 0.40% for $\xi K \gg 1$.

2. Modification to Linewidth Obtained for Different Correlation Functions

Swinney and co-workers[11,25] have modified the Kawasaki theory for different correlation functions:

$$\hat{G}_1(K) \propto \sin[(1-\eta)\arctan(K\xi)]/K(K^2+\xi^{-2})^{(1-\eta)/2} , \tag{9a}$$

$$\hat{G}_2(K) \propto (K^2+\xi^{-2})^{-(1-\eta/2)} , \tag{9b}$$

$$\hat{G}_3(K) \propto (\xi^{-2}+\phi^2K^2)^{\eta/2}/[\xi^{-2}+(1+\tfrac{1}{2}\eta\phi^2)K^2] . \tag{9c}$$

With an assumed $\eta = 0.1$ and $\phi = 0.5$ (or 0.1), they obtained an increase in the computed linewidth varying from 1–11% at $K\xi \ll 1$ and about 4–6% at $K\xi \gg 1$. Table V lists the percent change of Γ at $K\xi = 0.1$, 1, and 10 for Eq. (9).

3. Corrections due to Nonlocal Shear Viscosity

Kawasaki and Lo have removed the ambiguity associated with the so-called "high-frequency" shear viscosity[13] in Eq. (3) by considering the nonlocal shear viscosity which depends upon $K\xi$ as well as temperature. The so-called high-frequency viscosity η^*_{hf} is related to the macroscopic shear viscosity $\eta^*(T)$ by

$$\eta^*_{hf} = [H_0(K\xi)/H(K\xi)]\eta^*(T) . \tag{10}$$

The correction is quite important, amounting to about 30% for $K\xi = 20$, and remains finite ($\sim 5.5\%$) even in the hydrodynamic region. Values of $H(K\xi)/H_0(K\xi)$ at $K\xi = 0.1$, 1, and 10 are also listed in Table V. In the hydrodynamic limit, both the correlation function and nonlocal viscosity corrections contribute an approximate 5% change in the computed linewidth. With the vertex correction, either correlation function or nonlocal viscosity is sufficient to account for the discrepancy between experiments and theory. However, in the critical region, $\eta^*/\bar{\eta}^*_{hf} \simeq 1.25$. Thus, the main correction term must be contributions due to nonlocal viscosity. From Table V, for $K\xi = 0.1$ and 10, $H(K\xi)/H_0(K\xi) = 1.055$ and 1.23, and $\eta^*/\bar{\eta}^*_{hf}$ (measured) = 1.070 and 1.25, respectively. By means of Eq. (10), we see that the agreement between experiments ($\eta^*/\bar{\eta}^*_{hf}$) and the modified Kawasaki theory [$H(K\xi)/H_0(K\xi)$] is within 2%. The implication could be that deviation from the approximate Ornstein–Zernike correlation function must be small, and η and ϕ are small numbers if they exist. Figure 7 shows a comparison of the modified linewidth function

TABLE V. Percent change of computed linewidth due to vertex correlation function and nonlocal viscosity corrections.

	Modification	% change of Γ[a] $K\xi = 0.1$	1	10
1.	Vertex correction	−2.44		0.40
2.	Correlation functions	($\eta = 0.1$)		
	G_1 [Eq. (9a)]	11.1	9.5	6.2
	G_2 [Eq. (9b)]	7.6	7.0	5.7
	G_3 [Eq. (9c)] $\phi = 0.5$	3.7	4.3	5.6
	G_3 [Eq. (9c)] $\phi = 0.1$	1.0	1.2	4.4
3.	Nonlocal viscosity			
	$H(K\xi)/H_0(K\xi)$	5.5	7.0	23[b]
	$\eta^*/\bar{\eta}^*_{hf}$ (before correction)	7.0		25
	η^*/η^*_{hf} [after correction with (1) and (3)]	+3.9		+1.6
	η^*/η^*_{hf} [after corrections with (1)–(3)]			
	with G_1	−7.16		−4.6
	G_2	−3.66		−4.1
	$G_3(\phi = 0.5)$	0.24		−4.0
	$G_3(\phi = 0.1)$	2.94		−2.8

[a]The errors for η^*/η^*_{hf} in % change of Γ should be at least ± 1. Thus, figures after the decimal are not meaningful.

[b]Note: We have taken $H(K\xi)/H_0(K\xi) = 1.23$ at $K\xi = 10$ while $\bar{\eta}^*_{hf}$ is averaged over a range of $K\xi \leq 11$. Thus, in the critical region, we see that the correlation-function correction is needed even though it is likely to be small with $\eta < 0.1$ and ϕ small, if any.

$$\Gamma_K = (k_B T/6\pi\eta^*\xi^3)\, H(K\xi) \tag{11}$$

with our experimental data. Note that no adjustable parameters enter the theoretical curve. The measured linewidths are compared with Eq. (11) which can be computed using hydrodynamic shear viscosity by the capillary method and correlation length by the angular dissymmetry method. Higher-order effects appear to be unimportant since we have already achieved good agreement between experiments and theory. The background contribution (if any), the correlation-function modification, and the vertex correction play only secondary roles, or there could be effects cancelling one another. The solid line represents $H(K\xi)k_B T/(6\pi\xi^3K^3)$, where the $H(K\xi)$ function is obtained by computing $H_0(K\xi)$ from Eq. (4) and $H(K\xi)/H_0(K\xi)$ from Fig. 3 of Ref. 13. In terms of the reduced variable ($K\xi$), the computed curve should be valid for all systems. The solid circles represent experimental data for the isobutyric-acid–water system where Γ is obtained from Rayleigh linewidth studies, η^* is computed using Eq. (5), with $E = 0.27$, $F = -10.0$, $G = 1.35$, and $\alpha = -0.117$, and ξ by means of Eq. (7). The solid triangles represent typical data for the 3-methyl pentane-nitroethane system.[10] The agreement among the two experiments and the modified Kawasaki theory is remarkable. However, in the nonlocal hydrodynamic region, we note that

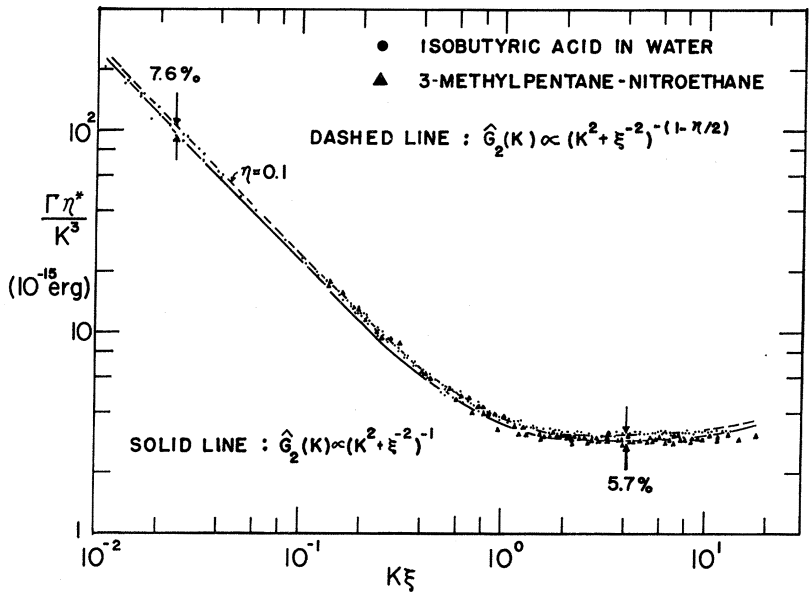

FIG. 7. Plot of $\ln(\Gamma/K^3)\eta^*$ vs $\ln K\xi$. Solid circles represent experimental data for the isobutyric-acid-water system. The parameters used are $A = 1.06\times10^{-13}$ cm^3/sec, $\nu = 0.613$, and $\xi_0 = 0.357\times10^{-7}$ cm. The solid curve represents Eq. (11); which includes the nonlocal viscosity correction but not the correlation function and vertex corrections. The dashed line represents $C(K\xi)\times$ Eq. (11), where $C(K\xi)$ accounts for the deviation of the Ornstein-Zernike correlation function but not the vertex correction. The solid triangles represent typical experimental data for the three-methyl pentane-nitroethane system from Fig. 3 of Ref. 10.

the measured data are higher than the computed curve which contains no adjustable parameters. Thus, it becomes necessary to consider a breakdown of the Ornstein–Zernike form of the correlation function. Any of the correlation functions in Eq. (9) will contribute to an increase in the computed curve. Since the vertex correction[12] provides a decrease in the computed linewidth in the hydrodynamic limit, we estimate $\eta \leq 0.1$ in order to account for the discrepancy. In the critical region, the values for the 3-methyl pentane-nitroethane appear a bit too low. There is a possibility that the capillary method becomes less reliable in the critical region because of gravitational effects at small temperature distances from the critical mixing point. It should be noted that the exponent α depends strongly upon the mathematical representation of the power law used. For example, the expression $\eta^* = Ae^{-\alpha} + \eta^*_{id}$ can also fit our experimental data. However, we may safely conclude that the viscosity anomaly is weak and the possibility of a cusp clearly exists even though the precision of present-day experimental data is not able to rule out a very weak power law or logarithmic divergence. A possible indirect evidence on the sharp-cusp formation very near the critical point is the slowing down in the collapse of the linewidth as the critical point is approached. Thus, for the isobutyric-acid–water system, we have used values of the hydrodynamic shear viscosity computed by means of Eq. (5) which was least-squares fitted using experimental data without those measured very near the critical mixing point ($T - T_c \leq 0.05\,^\circ$C). The discrepancy between the isobutyric-acid–water system and the modified Kawasaki theory can be reduced if we utilize the correlation-function modification, as shown by the dotted line in Fig. 7. This dotted line represents $H(K\xi)C(K\xi)k_BT/(6\pi\xi^3K^3)$, where $C(K\xi)$ is the correction factor which takes into account the correlation-function modification. [Eq. (9b) with $\eta = 0.1$].[25] There are two remarks worthwhile mentioning. First, we are considering discrepancies of only a few percent. Thus, the conclusions from those comparisons must necessarily be on a less-solid footing. Second, with precise experimental data, we see a new method of determining the form of the correlation function by comparing data with theory over the entire $K\xi$ range. However, such a new approach cannot yet be utilized until the modified Kawasaki theory, which already includes vertex, correlation functions, and nonlocal viscosity corrections, is further improved. In Fig. 7, the measured data at $K\xi > 1$ level off faster than the computed curve even though the discrepancy can hardly be detected in such an insensitive log-log plot.

A more crucial comparison is achieved by plotting $\eta^*(T)/\eta^*_{hf}$ vs $\ln K\xi$, as shown in Fig. 8. The measured points are computed according to the expression

$$\eta^*_c(T)/\eta^*_{hf} = 6\pi\eta^*_c(T)\xi^3\Gamma/k_BT\,H_0(K\xi)\ , \qquad (12)$$

where $\eta^*_c(T)$ is the computed hydrodynamic shear viscosity from Eq. (5), with $E = 0.27$, $F = -10.0$, $G = 1.35$, and $\alpha = 0.117$. Γ is the measured Rayleigh linewidth, $\xi = \xi_0\epsilon^{-\nu}$ with $\xi_0 = 0.357\times10^{-7}$ cm and $\nu = 0.613$. $H_0(K\xi)$ is computed by means of Eq. (4). The solid line represents $H(K\xi)/H_0(K\xi)$ which is identical to Fig. 3 of Ref. 13.

In Fig. 8 the absence of adjustable parameters suggests that while the agreement between experi-

ments and theory is already exceedingly good, further modification of the theory is needed since the discrepancies exceed the combined error limits of our measurements. The solid curve (H/H_0) falls consistently below the measured points over the entire $K\xi$ range till $K\xi \gg 1$. Contribution of the simplest vertex correction for the computed linewidth is -2.44% in the hydrodynamic region and 0.40% in the critical region.[12] Thus, according to Fig. 8, the computed curve needs to be raised about another 7% at small values of $K\xi$ and not so much in the critical region if we take Eq. (12) as the definition for η^*_{hf}. The dotted line in Fig. 8 represents $(H/H_0)C(K\xi)$, where $C(K\xi)$ is the correlation-function correction [using Eq. (9b) with $\eta = 0.1$].[25] Hence, if we take into account the vertex correction as well as the correlation-function modification in addition to the nonlocal viscosity effect, we can obtain excellent agreement between experiments and theory over large ranges of $K\xi$ up to $K\xi \sim 1$.

The quantity H/H_0 should be independent of the nature of the fluid systems under investigation. The solid triangles in Fig. 8 represent typical data (η^*/η^*_{hf}) for the 3-methyl pentane-nitroethane syste tem.[10] Aside from imprecisions in computing data from graphs in the literature, we believe that our linewidth measurements are better because of signal correlation rather than spectrum analysis. Nevertheless, the agreement is quite remarkable over the $K\xi$ range from the hydrodynamic region to about $K\xi \sim 1$ for both systems with the modified theory.

In the critical region, especially at large values of $K\xi$, the 3-methyl pentane-nitroethane system shows lower values of η^*/η^*_{hf} than expected. The values become even lower if we take the earlier

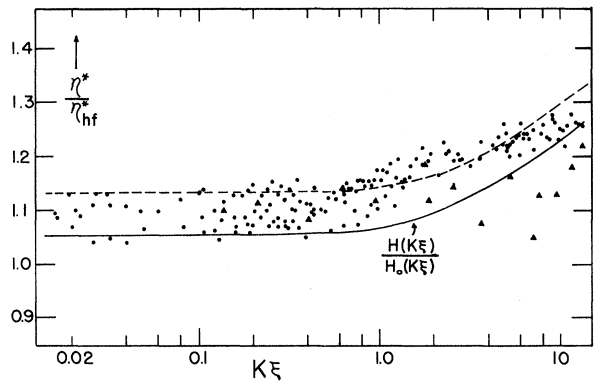

FIG. 8. Plot of η^*/η^*_{hf} vs $\ln K\xi$. $\eta^*/\eta^*_{hf} = 6\pi\eta^*\xi^3\Gamma/k_BTH_0$. Solid line represents H/H_0. Dotted line represents $(H/H_0)C(K\xi)$ with $\eta = 0.1$. ●: isobutyric-acid–water system; ▲: three-methyl pentane-nitroethane system.

hydrodynamic shear viscosity data. The source of this discrepancy could be partly due to lower values in the measured hydrodynamic shear viscosity in the critical region as discussed earlier. Similarly, for the isobutyric-acid–water system, η^*/η^*_{hf} has lower values in the critical region if we used the measured hydrodynamic shear viscosity instead of Eq. (5). We believe that the correct values for the hydrodynamic shear viscosity in the critical region are slightly higher than those reported in the literature.[17] On the other hand, the shape of the measured curve in Fig. 8 is not sensitive to the magnitudes of ξ_0 and ν in the critical region $(K\xi > 1)$. Thus, we observe a discrepancy between experiments and theory even if we neglect considerations of η^*/η^*_{hf} in the large ranges of $K\xi$ corresponding to $T - T_c < 0.01$ for the hydrodynamic shear viscosity where gravitational effects are likely to be significant. This leveloff effect in the shape of the measured data at $K\xi > 1$ cannot be taken into account by (a) the simple vertex correction, (b) the correlation-function correction, and (c) the nonlocal viscosity correction. It is not likely because of gravitational effects since we have neglected the measured hydrodynamic shear viscosity very near the critical mixing point nor because of slight variations in the magnitudes of ξ_0 and ν.

The $H(K\xi)$ function of Kawasaki and Lo[13] can be tested on a relative scale in the absence of hydrodynamic-shear-viscosity data.[26] At a given temperature, the hydrodynamic shear viscosity $\eta^*(T)$ and the long-range correlation length $\xi(T)$ are constant. Then, the ratio of Rayleigh linewidth at two different scattering angles, say $\theta = 40°$ and $130°$, is

$$\frac{\Gamma_K(130°)}{\Gamma_K(40°)} = \frac{H_0[K(130°)\xi]}{H_0[K(40°)\xi]} \equiv \frac{H_{0,130}}{H_{0,40}} \tag{13}$$

according to Eq. (3), where η^*_{hf} is assumed to be independent of $K\xi$; or

$$\frac{\Gamma_K(130°)}{\Gamma_K(40°)} = \frac{H[K(130°)\xi]}{H[K(40°)\xi]} \equiv \frac{H_{130}}{H_{40}} \tag{14}$$

according to Eq. (11). Equation (13) remains valid even if η^*_{hf} depends upon temperature. $H(K\xi)/H_0(K\xi)$ increases rapidly for large values of $K\xi$ and remains relatively constant in the hydrodynamic region. Far away from the critical point, both $K(40°)\xi$ and $K(130°)\xi$ are in the hydrodynamic region. Thus, $H_{0,130}/H_{0,40}$ and H_{130}/H_{40} coincide. At smaller temperature distances, $K(130°)\xi$ is further into the critical region than $K(40°)\xi$. Then, $H_{0,130}/H_{0,40}$ deviates from H_{130}/H_{40} as shown in Fig. 9. We have used two different values of ξ_0 and ν to illustrate the fact that the comparison remains valid even if our measured values of ξ_0

(= 3.57 Å) and ν (= 0.613) are slightly different from the correct ones. From universality considerations,[27] the most probable value for ν could be 0.63. We then compute a ξ_0 value by assuming $\nu = 0.63$ in $\xi = \xi_0 \epsilon^{-\nu}$ at $T - T_c = 0.1\,^\circ$C. In Fig. 9, the data appear to agree better with the modified theory of Kawasaki and Lo[13] even though deviations at large values of ξ exist. The lower value of $\Gamma(130^\circ)/\Gamma(40^\circ)$ when compared with H_{130}/H_{40} at $\xi \sim 10^3$ Å seems to indicate that the ratio of $H(K\xi)/H_0(K\xi)$ increases too fast at large values of $K\xi$.

Figure 10 shows deviation plots of $(\Gamma_{expt} - \Gamma_{th})/\Gamma_{expt}$ vs $\ln K\xi$, where Γ_{expt} represents the measured Rayleigh linewidth and Γ_{th} is computed from Eq. (11). In Fig. 10(a), $\nu = 0.613$ and $\xi_0 = 3.57$ Å, while $\nu = 0.63$ and $\xi_0 = 3.11$ Å in Fig. 10(b). The first (ξ_0, ν) pair is the best values from least-squares fit of intensity measurements using $\lambda_0 = 435.8$ nm. The second (ξ_0, ν) pair is again introduced by assuming $\nu = 0.63$. The values of ξ_0 and ν seem to influence the magnitude of Γ_{th} at small values of $K\xi$ and become insensitive at large values of $K\xi$. In order to take into account the vertex and correlation-function corrections as well as the contribution from nonlocal viscosity, we need to observe the deviations over the entire $K\xi$ range. In Fig. 10(a), at small $K\xi$ values ($K\xi \leq 1$), $(\Gamma_{expt} - \Gamma_{th})/\Gamma_{expt}$ is about +6%. With −2.44% due to the vertex contribution in the hydrodynamic limit, it requires a correlation function of Eq. (9b) with $\eta < 0.1$ to account for the discrepancy. Other effects, such as the frequency dependence of the viscosity, need to be included since the deviation drops off too fast at large values of $K\xi$. The maximum in Fig. 10 cannot be explained by the presently known theoretical modification as we have already discussed. Experimentally, it is not likely that any appreciable error exists in our Rayleigh linewidth measurements. The magnitude of ξ does not change the qualitative behavior as shown by Figs. 10(a) and 10(b). There could be possible errors in the hydrodynamic shear-viscosity studies. Nevertheless, we believe that we have alleviated part of the difficulties by utilizing Eq. (5). Thus, further improvements of the modified Kawasaki–Lo theory should be worthwhile.

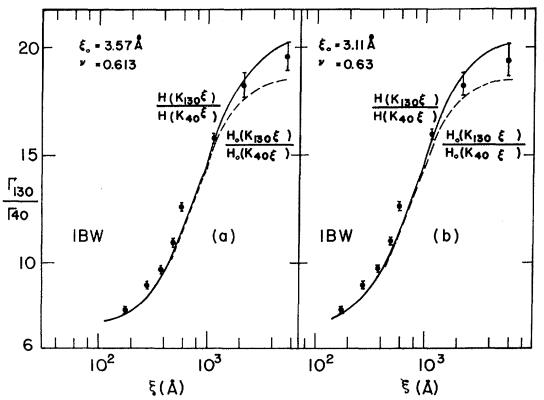

FIG. 9. (a) A comparison of ratio of Rayleigh linewidth as a function of correlation length with theories of Kawasaki and Lo (Ref. 13) and Kawasaki (Ref. 7) using $\xi_0 = 3.57$ Å and $\nu = 0.613$. (b) The same comparison using $\xi_0 = 3.11$ Å and $\nu = 0.63$ obtained by equating $\xi = \xi_0 \epsilon^{-0.63}$ at $T - T_c = 0.1\,^\circ$C. No correlation-function and vertex corrections have been included. The experimental data agree better with the modified theory of Kawasaki and Lo (Ref. 13). Note that the general behavior is relatively independent of small changes in the magnitudes of ξ_0 and ν.

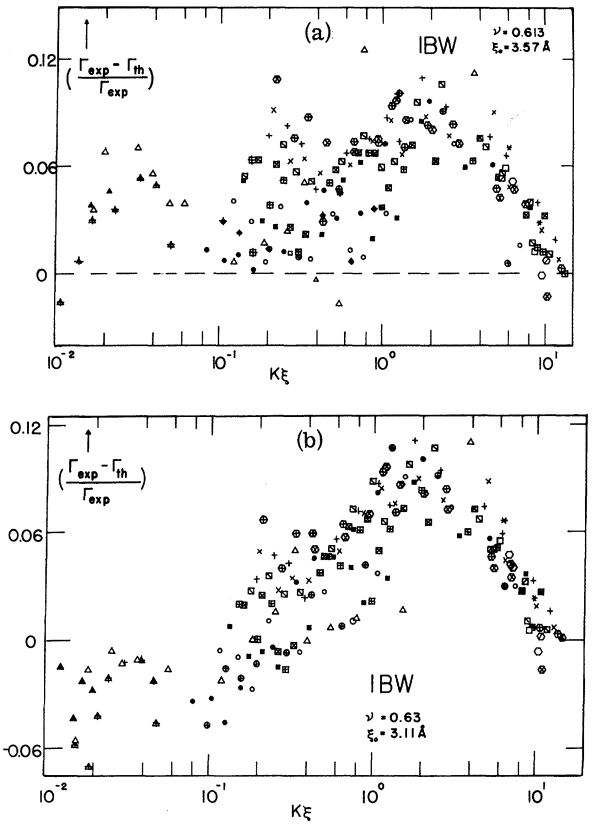

FIG. 10. (a) Plot of $(\Gamma_{expt} - \Gamma_{th})/\Gamma_{expt}$ vs $\ln K\xi$. Γ_{expt} represents the measured linewidth. Γ_{th} is computed from Eq. (11) using $\xi_0 = 0.357 \times 10^{-7}$ cm; $\nu = 0.613$; η^* from Eq. (5) with $E = 0.27$, $F = -10.0$, $G = 1.35$, and $\alpha = -0.117$; $H_0(K\xi)$ from Eq. (4); and $H(K\xi)/H_0(K\xi)$ from Fig. 3 of Ref. 13. The following symbols denote various scattering angles θ: ▲, 20°; ⏃, 25°; △, 30°; ●, 40°; ⊕, 50°; ○, 60°; ■, 70°; ⊞, 80°; ⊠, 90°; ⊡, 95°; ⧅, 100°; □, 105°; +, 110°; *, 115°; ×, 120°; ⧲, 125°; ⊕, 130°; ⊘, 135°; ⊗, 140°. (b) The same plot using $\xi_0 = 0.311 \times 10^{-7}$ cm and $\nu = 0.63$.

IV. SUMMARY AND CONCLUSIONS

A careful comparison of linewidth, angular dissymmetry, and hydrodynamic shear-viscosity data

of a critical binary-liquid mixture with the mode-mode coupling theory of Kawasaki has led to the following remarks:

(i) The high-frequency shear viscosity η^*_{hf} depends upon $K\xi$ (as well as temperature) in the critical region.

(ii) η^*_{hf} depends upon temperature, and in the hydrodynamic limit, it exhibits a similar temperature behavior as the hydrodynamic shear viscosity $\eta^*(T)$. A cusp behavior in the critical viscosity anomaly is strongly indicated.

(iii) $\eta^* > \eta^*_{hf}$ over the entire $K\xi$ range.

(iv) The formula ΓAK^3 seems to hold very well even though η^*_{hf} depends upon $K\xi$. Implicitly, this could mean that the $K\xi$ dependence of η^*_{hf} is not very strong.

(v) Equation (3) assumes that η^*_{hf} is a constant, independent of $K\xi$ and T. If we force a three-parameter fit using only the linewidth data, we obtain a set of values of ξ_0, ν, and A(or η^*_{hf}) which are not consistent over different ranges of $K\xi$ and with angular dissymmetry and viscosity studies. Thus, it is incorrect to analyze experimental data using this approach and to proclaim a good agreement between experiments and theory.

(vi) $D \neq k_B T/6\pi\eta^*\xi$ since we have shown that $\eta^*_{hf} \neq \eta^*$.

(vii) It is invalid to obtain the long-range correlation length by means of Eq. (2) because η^*_{hf} depends upon $K\xi$. The ratio of slope/intercept in a Γ/K^2-vs-K^2 plot will be slightly distorted. As a result, temperature dependence of the long-range correlation length is incorrect if we use Eq. (2) in the nonlocal hydrodynamic region. Table IV clearly demonstrates that the factor $\frac{3}{5}$ is valid only over limited $K\xi$ and temperature ranges.

(viii) $D \neq D_0\epsilon^{\gamma^*}$. The critical exponent γ^* is obviously an apparent one. The viscosity term has a complex temperature dependence. With $D = k_B T/6\pi\eta^*_{hf}\xi$, it is not reasonable to use a single critical exponent γ^* to represent the temperature dependence of the diffusion coefficient over large temperature distances as shown in Fig. 4.

(ix) Fluctuations in data points which are outside of our error limits in a plot of $\eta^*(T)/\eta^*_{hf}$ vs $K\xi$ or Fig. 8 reveal additional possible weaknesses in the theory. It should be noted that such fluctuations are relatively independent of scattering angles or temperatures studied. Thus, there are other effects which have to be taken into account in the modified theory.[28]

(x) The maximum in Fig. 10($1 \leq K\xi \leq 10$) cannot be explained. We believe that the slight increase up to $K\xi \sim 3$ is real. Such discrepancies in this region could be taken into account by means of the correlation-function modification and vertex corrections. The decrease for $K\xi \geq 4$ means that the computed H/H_0 curve increases too fast at large values of $K\xi$, suggesting a frequency dependence of the high-frequency shear viscosity.

(xi) Values of reported hydrodynamic shear viscosities at very small temperature distances are questionable.[17,29]

(xii) With good experimental data in linewidth, angular dissymmetry, and hydrodynamic shear viscosity, the theory of Kawasaki and Lo[13] after *further* modifications suggests another interesting method of eventually determining the form of the correlation functions with their corresponding critical exponents by comparing experiments with theory over the entire $K\xi$ range.

(xiii) It should be noted that the correlation-function correction for the original Kawasaki theory was computed by Swinney and Saleh.[25] The modified Fisher formula with the exponent η is expected to be valid at $K\xi \gg 1$ and theoretical linewidth change may be different with different correlation functions in the critical region. However, in the hydrodynamic region, Swinney, Henry, and Cummins[11] and Swinney and Saleh[25] predicted equivalent changes in linewidths dependent upon the magnitudes of critical exponents η and ϕ and a lack of convergence with the computed linewidth using the Ornstein–Zernike correlation function. In our discussion, we have simply used their yet unpublished results in Table V, and Figs. 7 and 9 without repeating the numerical calculations.

(xiv) Recently, Perl and Ferrell[30] proposed that retardation produces some non-Lorentzian distortion in the diffusion line shapes which we have been unable to observe with our present instrumentation. Perhaps, as they have mentioned, the effect is too weak to be detected experimentally.

ACKNOWLEDGMENTS

The authors would like to thank Professor H. L. Swinney for sending us the numerical computation of the correlation-function corrections. Financial support of this research by the National Science Foundation and donors of the Petroleum Research Fund, administered by the American Chemical Society is gratefull acknowledged.

---

†Author to whom requests for reprints should be addressed.

[1]S. S. Alpert, Y. Yeh, and E. Lipworth, Phys. Rev. Letters 14, 486 (1965).

[2]P. Debye, Phys. Rev. Letters 14, 783 (1965).

[3]L. Landau and G. Placzek, Physik. Z. Sowjetunion 5, 172 (1934).

[4]M. Fixman, *Pontifica Academic Scientiarum Scripta Varia* 31 *on Molecular Forces* (Pontifical Academy of Science, Vatican City, Italy, 1966), p. 329; W. D.

Botch, Ph. D. thesis (University of Oregon, 1963) p. 63, (unpublished).

[5]B. U. Felderhof, J. Chem. Phys. 44, 602 (1966).

[6]L. P. Kadanoff and J. Swift, Phys. Rev. 166, 89 (1968); J. Swift, *ibid.* 173, 257 (1968).

[7]K. Kawasaki, Phys. Letters 30A, 325 (1969); Ann. Phys. (N. Y.) 61, 1 (1970); Phys. Rev. A 1, 1750 (1970); in *Proceedings of the International Summer School of Physics "Enrico Fermi," Varenna, Italy*, 1970 (Academic, New York, to be published).

[8]B. Chu, Ber. Bunsenges Physik. Chem. 76, 202 (1972).

[9]B. Chu, D. Thiel, W. Tscharnuter, and D. V. Fenby, J. Phys. Suppl. 33, 111 (1972).

[10]R. F. Chang, P. H. Keyes, J. V. Sengers, and C. O. Alley, Phys. Rev. Letters 27, 1706 (1971).

[11]H. L. Swinney, D. L. Henry, and H. Z. Cummins, J. Phys. Suppl. 33, 81 (1972).

[12]S. M. Lo and K. Kawasaki, Phys. Rev. A 5, 421 (1972).

[13]K. Kawasaki and S.-M. Lo, Phys. Rev. Letters 29, 48 (1972).

[14]B. Chu, Ann. Rev. Phys. Chem. 21, 145 (1970).

[15]B. Chu, F. J. Schoenes, and W. P. Kao, J. Am. Chem. Soc. 90, 3042 (1966).

[16]D. Woermann and W. Sarholz, Ber. Bunsenges. Physik. Chem. 69, 319 (1965).

[17]J. C. Allegra, A. Stein, and G. F. Allen, J. Chem. Phys. 55, 1716 (1971).

[18]S. P. Lee, W. Tscharnuter, and B. Chu, Phys. Rev. Letters 28, 1509 (1972).

[19]B. Chu, J. Chem. Phys. 47, 3816 (1967).

[20]W. Tscharnuter, D. Thiel, and B. Chu, Phys. Letters 38A, 299 (1972).

[21]For example, the technique by P. N. Pusey and W. I. Goldburg [Phys. Rev. A 3, 766 (1971)] consists of measurements of one delay point at a time. Similarly, if we use a General Radio 1900 wave analyzer, a good linewidth measurement takes about 3 h with about one-tenth the precision, while our present technique takes between 5–20 min.

[22]B. I. Halperin and P. C. Hohenberg, Phys. Rev. 177, 952 (1969).

[23]R. A. Ferrell, Phys. Rev. Letters 24, 1169 (1970).

[24]M. E. Fisher, Rept. Progr. Phys. 30, 615 (1967).

[25]H. L. Swinny and B. A. Saleh (unpublished).

[26]C. C. Lai and S. H. Chen, Phys. Rev. Letters 29, 401 (1972).

[27]B. Chu, J. Status Phys. (to be published).

[28]M. E. Fisher and R. J. Burford, Phys. Rev. 156, 583 (1967).

[29]H. M. Leister, J. C. Allegra, and G. F. Allen, J. Chem. Phys. 55, 4265 (1971).

[30]R. Perl and R. A. Ferrell, Phys. Rev. Letters 29, 51 (1972).